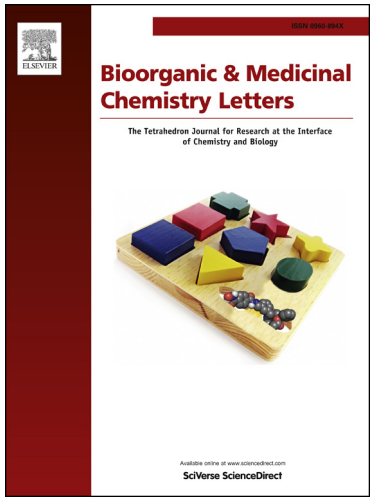

The imidazo[1,2-*a*]pyridine ring system as a scaffold for potent dual phosphoinositide-3-kinase (PI3K)/mammalian target of rapamycin (mTOR) inhibitors

Markian M. Stec, Kristin L. Andrews, Yunxin Bo, Sean Caenepeel, Hongyu Liao, John McCarter, Erin L. Mullady, Tisha San Miguel, Raju Subramanian, Nuria Tamayo, Douglas A. Whittington, Ling Wang, Tian Wu, Leeanne P. Zalameda, Nancy Zhang, Paul E. Hughes, Mark H. Norman

PII: S0960-894X(15)00840-9
DOI: http://dx.doi.org/10.1016/j.bmcl.2015.08.016
Reference: BMCL 23010

To appear in: *Bioorganic & Medicinal Chemistry Letters*

Received Date: 13 June 2015
Revised Date: 2 August 2015
Accepted Date: 6 August 2015

Please cite this article as: Stec, M.M., Andrews, K.L., Bo, Y., Caenepeel, S., Liao, H., McCarter, J., Mullady, E.L., Miguel, T.S., Subramanian, R., Tamayo, N., Whittington, D.A., Wang, L., Wu, T., Zalameda, L.P., Zhang, N., Hughes, P.E., Norman, M.H., The imidazo[1,2-*a*]pyridine ring system as a scaffold for potent dual phosphoinositide-3-kinase (PI3K)/mammalian target of rapamycin (mTOR) inhibitors, *Bioorganic & Medicinal Chemistry Letters* (2015), doi: http://dx.doi.org/10.1016/j.bmcl.2015.08.016

Graphical Abstract

To create your abstract, type over the instructions in the template box below.
Fonts or abstract dimensions should not be changed or altered.

The imidazo[1,2-*a*]pyridine ring system as a scaffold for potent dual phosphoinositide-3-kinase (PI3K)/mammalian target of rapamycin (mTOR) inhibitors

Leave this area blank for abstract info.

Markian M. Stec,* Kristin L. Andrews, Yunxin Bo, Sean Caenepeel, Hongyu Liao, John McCarter, Erin L. Mullady, Tisha San Miguel, Raju Subramanian, Nuria Tamayo, Douglas A. Whittington, Ling Wang, Tian Wu, Leeanne P. Zalameda, Nancy Zhang, Paul E. Hughes, and Mark H. Norman

18

PI3Kα K_i = 11 nM

mTOR IC_{50} = 206 nM

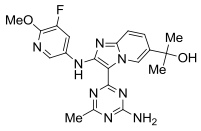

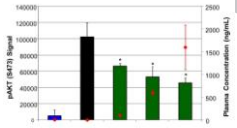

Bioorganic & Medicinal Chemistry Letters
journal homepage: www.elsevier.com

The imidazo[1,2-*a*]pyridine ring system as a scaffold for potent dual phosphoinositide-3-kinase (PI3K)/mammalian target of rapamycin (mTOR) inhibitors

Markian M. Stec[a,*], Kristin L. Andrews[d], Yunxin Bo[a], Sean Caenepeel[b], Hongyu Liao[a], John McCarter[e], Erin L. Mullady[f], Tisha San Miguel[e], Raju Subramanian[c], Nuria Tamayo[a], Douglas A. Whittington[d], Ling Wang[b], Tian Wu[g], Leeanne P. Zalameda[e], Nancy Zhang[b], Paul E. Hughes[b], and Mark H. Norman[a]

[a]*Department of Medicinal Chemistry, Amgen Inc., One Amgen Center Drive, Thousand Oaks, California 91320-1799, USA*
[b]*Department of Oncology, Amgen Inc., One Amgen Center Drive, Thousand Oaks, California 91320-1799, USA*
[c]*Department of Pharmacokinetics and Drug Metabolism, Amgen Inc., One Amgen Center Drive, Thousand Oaks, California 91320-1799, USA*
[d]*Department of Molecular Structure, Amgen Inc., One Amgen Center Drive, Thousand Oaks, California 91320-1799, USA and 360 Binney St., Cambridge, Massachusetts 02142, USA*
[e]*Department of High-Throughput Screening/Molecular Pharmacology, Amgen Inc., One Amgen Center Drive, Thousand Oaks, California 91320-1799, USA*
[f]*Department of High-Throughput Screening / Molecular Pharmacology, Amgen Inc., 360 Binney Street, Cambridge, Massachusetts 02142*
[g]*Department of Basic Pharmaceutics, Amgen Inc., One Amgen Center Drive, Thousand Oaks, California 91320-1799, USA*

ARTICLE INFO

Article history:
Received
Revised
Accepted
Available online

Keywords:
Phosphoinositide 3-kinase
Imidazo[1,2-*a*]pyridine
Ribose pocket
Affinity pocket
Kinase inhibitor
mTOR

ABSTRACT

Based on lead compound **1**, which was discovered from a high-throughput screen, a series of PI3Kα/mTOR inhibitors were evaluated that contained an imidazo[1,2-*a*]pyridine as a core replacement for the benzimidazole contained in **1**. By exploring various ring systems that occupy the affinity pocket, two fragments containing a methoxypyridine were identified that gave <100 nM potency toward PI3Kα in enzyme and cellular assays with moderate stability in rat and human liver microsomes. With the two methoxypyridine groups selected to occupy the affinity pocket, analogs were prepared with various fragments intended to occupy the ribose pocket of PI3Kα and mTOR. From these analogs, tertiary alcohol **18** was chosen for in vivo pharmacodynamic evaluation based on its potency in the PI3Kα cellular assay, microsomal stability, and in vivo pharmacokinetic properties. In a mouse liver pharmacodynamic assay, compound **18** showed 56% inhibition of HFG-induced AKT (Ser473) phosphorylation at a 30 mg/kg dose.

The study of phosphoinositide 3-kinases (PI3Ks) dates back to the 1980s with publications from multiple research groups on the phosphorylation of phosphatidylinositol at the 3-hydroxyl position through kinase activity.[1-4] Since that time, various classes of PI3Ks have been elucidated including class I, II, and III that differ in their structural characteristics and substrate specificity. The class I PI3Ks are further divided into class Ia, which include PI3Kα, β, and δ, and the class Ib subgroup which includes PI3Kγ. When class I PI3Ks are activated, a signal transduction cascade leads to the phosphorylation of AKT (also known as PKB). Phosphorylated AKT mediates multiple cellular functions including cell cycle progression, survival, transcription, and glycogen synthesis.[5,6]

Approximately 20 years after these initial discoveries, definitive links between PI3Kα and cancer were identified when mutations of the oncogene, PIK3CA, which encodes the catalytic subunit of PI3Kα, p110α, were found to be one of the most common mutations in human solid tumors.[7,8] Numerous PI3K inhibitors have been developed that have shown preclinical tumor growth inhibition with varying selectivity profiles from PI3Kα isoform-selective to pan-class I PI3K-selective to dual PI3K/mTOR compounds.[9-13] Mammalian target of rapamycin (mTOR) is a PI3K-related kinase (PIKK) in the PI3K/AKT pathway, which integrates signals from growth factors and nutrients, and is also an important enzyme involved in the promotion of cancer cell growth and survival.[14,15] At least seven dual PI3K/mTOR inhibitors, six pan-PI3K inhibitors, and ten isoform-selective PI3Kα inhibitors are in, or have completed, phase I or phase II clinical trials for cancer, either alone or in combination therapy.[16] It appears that the various tissue specific and compensatory mechanisms present in the PI3K/AKT pathway pose a challenge to patient and tumor type

* Corresponding author. Tel.: +1 805 447 8006 (O); fax: +1 805 480 3015.
E-mail address: mstec@amgen.com (M. M. Stec).

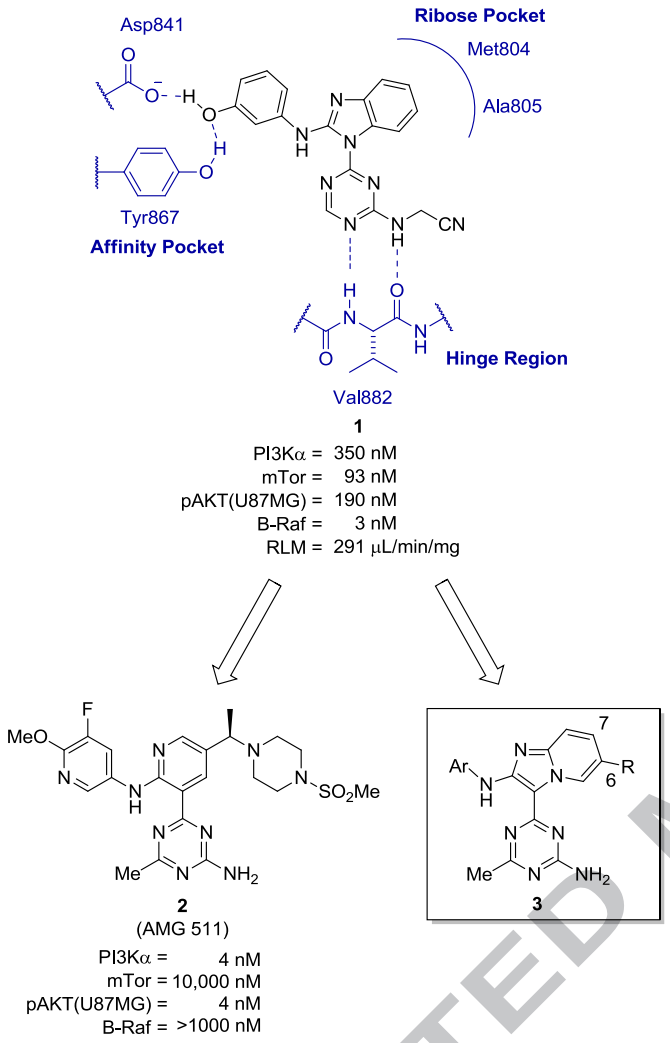

Figure 1. Lead compound **1** and PI3Kα series arising from **1**. Amino acid numbering reflects that of the PI3Kγ sequence.

selection; however, preliminary clinical benefits have been observed.[11-13,17-21]

We have previously reported the results of a high-throughput screening effort that identified benzimidazole-triazine **1** (Figure 1) to be a moderately potent inhibitor of PI3Kα (IC_{50} = 350 nM) and mTOR (IC_{50} = 93 nM).[22,23] Compound **1** also showed moderate potency in the U87 MG pAKT cellular assay; however, it was metabolically unstable and showed high in vitro clearance in rat liver microsomes (CL_{int} = 291 μL/min/mg). Rat bile duct cannulation studies determined that oxidation on the benzimidazole core was one route of metabolism.[23] In addition to poor metabolic stability, benzimidazole-triazine **1** was not selective over protein kinases such as B-raf (^{V600E}B-Raf IC_{50} = 3 nM). However, we believed that compound **1** was a reasonable lead as a PI3Kα inhibitor and, with X-ray co-crystal and modeling studies, we sought for ways to improve its potency, selectivity, and metabolic stability. One approach we have taken was to replace the benzimidazole core of **1** with 6-membered rings such as pyridine.[22,24] These modifications culminated in the discovery of clinical candidate **2** (AMG 511), which was a potent (PI3Kα = 4 nM) and selective (e.g., 2500-fold over mTOR and >250-fold over B-Raf) pan-PI3K inhibitor. Compound **2** was efficacious in the mouse U87 MG xenograft tumor growth inhibition model with an ED_{50} of 0.6 mg/kg.[24]

In addition to the successful pyridine core derivatives, alternative replacements to the benzimidazole core were sought that would provide metabolically stable yet potent and efficacious compounds. We postulated that the imidazo[1,2-*a*]pyridine core may provide the desired potency, efficacy, and stability and would also be amenable to the substitution patterns required for our established SAR. Therefore, this disclosure explores imidazo[1,2-*a*]pyridines as an alternative 5,6-heterocylic core utilizing information that has been acquired in our PI3Kα and mTOR[23,25] programs to discover potent and efficacious PI3Kα/mTOR dual inhibitors. The compounds described herein are represented by general structure **3**. This scaffold maintains the aminotriazine moiety to interact with the hinge region of the protein, utilizes aromatic amines (Ar) to occupy the affinity pocket, and provides a position on the imidazopyridine core (R) to incorporate groups to occupy the ribose pocket of PI3Kα.

At the time these studies were performed, structures of inhibitors bound in PI3Kα were, and still are, relatively rare and more difficult to obtain.[26-29] However, because of the high homology between PI3Kα and PI3Kγ, particularly at the ATP binding site, the use of PI3Kγ provided good correlation between observations made from crystallographic studies and experimentally observed SAR. An overlay of compounds **1** and **2** bound to PI3Kγ is shown in Figure 2. Two hydrogen bond interactions from the triazine to Val882 are present for both compounds in the "hinge region" of the kinase. In the affinity pocket region of the protein, a water molecule bridges the pyridine nitrogen of **2** with Asp841 and Tyr867 replacing the phenol group of **1**. This water molecule shifts the aromatic ring that occupies the affinity pocket away from Asp841 and Tyr867. The ribose pocket is minimally occupied in **1**, while compound **2** projects the piperazine methylsulfonamide moiety up towards the kβ3-kβ4 loop (P-loop) in a trajectory that is orthogonal to the core. The bicyclic nature of the benzimidazole core inherently projects further into the ribose pocket than the monocyclic pyridine core. As a result, we postulated that shorter substituents (e.g., without the benzylic methylene spacer) may be required to occupy the ribose pocket on an imidazopyridine core relative to a monocyclic pyridine core.

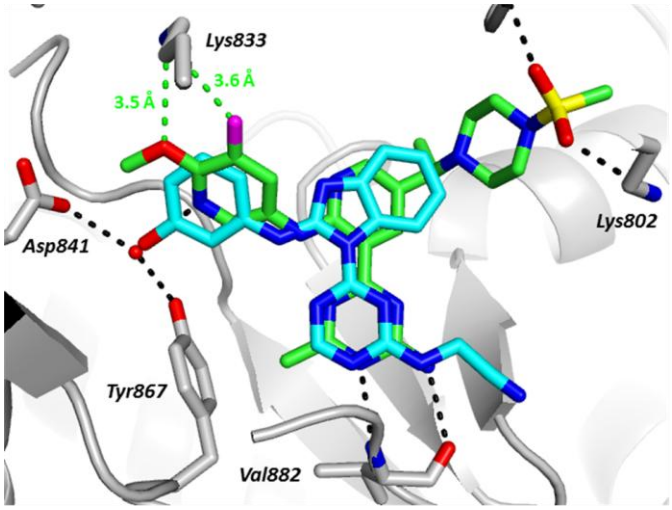

Figure 2. X-ray co-crystal structures of compounds **1** (blue) and **2** (AMG 511, green) in PI3Kγ (PDB codes 3QAQ and 4FLH, respectively).

The compounds described in this paper were screened in an in vitro AlphaScreen assay to determine PI3K inhibition of the four isoforms (α, β, γ, and δ) and mTOR.[30] Inhibition of the β, γ, and δ isoforms will only be reported for the compound that progressed into in vivo studies. Cellular activity was determined using a SureFire detection kit to measure downstream inhibition of AKT (Ser473) phosphorylation in U87 MG human glioblastoma cells.[31]

In our initial SAR investigations, we explored a select group of aromatic substituents that occupied the affinity pocket of the kinase with fragments that afforded potent analogs in the pyridine core series (Table 1). The 2-methoxypyridine substituted compound (**4**) showed good potency towards PI3Kα (29 nM), mTOR (37 nM) and in the pAKT cellular assay (40 nM). Replacing the methoxy group of **4** with an ethoxy group (compound **5**) resulted in a sixfold loss in potency in both the PI3Kα enzyme assay and cellular assay. This suggested that substituents could not be extended further into the affinity pocket. The 3-fluoro-2-methoxypyridine compound (**6**) showed a twofold gain in PI3Kα potency (14 nM) over **4**; however, potency in the cellular assay diminished modestly to 86 nM. Compound **6** did show some selectivity (14-fold) over mTOR.

Various 5,6- and 6,6-bicyclic groups were also explored in the affinity pocket region. These bicyclic heterocycles were selected to probe the hydrogen bonding network within the affinity pocket by placing nitrogen atoms at several different positions within these derivatives.[32] The isoquinoline, quinoline, and indazole analogs **8**, **9**, and **10** were found to be significantly more potent than quinoline **7** in the enzyme assay. By examining overlays of compounds **7**-**10** with **1**, it appears that compounds **8** and **9** can place the quinoline nitrogen in a similar position to the phenol oxygen of **1** in the affinity pocket compared to quinoline **7**. With the indazole analog **10**, modeling suggested that both indazole nitrogens projected towards Asp841 and Tyr867 thereby establishing a good hydrogen bonding network in the affinity pocket. Although the majority of these bicylic-heterocycle derivative showed good activity in the enzyme assay, compounds **8**, **9**, and **10** showed high microsomal clearance.[33]

Table 1. In vitro potency and microsomal stability of PI3Kα/mTOR inhibitors with an imidazopyridine core.

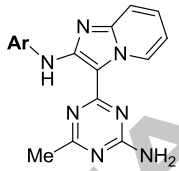

Compound	Ar	PI3Kα (K_i, nM)[a]	mTOR (IC_{50}, nM)[a]	pAKT (U87 MG) (IC_{50}, nM)[b]	Liver Microsomes (Cl_{int}, μL/min/mg)	
					Rat	Human
4	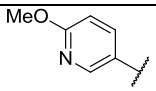	29	37	40	101	65
5	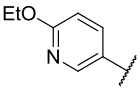	148	57	229	105	49
6	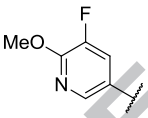	14	198	86	71	66
7	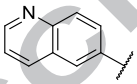	529	277	>780	62	111
8	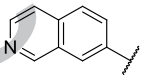	54	12	N/A	238	105
9	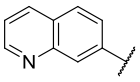	43	1.7	18	144	133
10	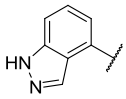	5.6	16	32	175	70

[a]Data represents an average of at least two determinations unless indicated otherwise. A statistical analysis of this data may be found in the supplementary material. [b]Data represents a single measurement.

Based on the potency and both rat and human microsomal stability found in compounds **4** and **6**,[34,35] a focused series of analogs was explored that contained the 2-methoxypyridine or the 3-fluoro-2-methoxypyridine fragment in the affinity pocket region of PI3Kα but that also contained an additional substituent intended to occupy the ribose pocket (Table 2). This substituent was included with the goal of improving potency and to potentially block sites of metabolism on the imidazopyridine ring system. As can be seen in the X-ray structures in Figure 2, the piperazine sulfonamide of compound **2** bisects the aromatic C-C

bond of the phenyl ring distal to the 5-membered ring. Therefore, based on crystal structure overlays, both the 6- and 7-positions of the imidazopyridine appeared to be viable options for the incorporation of ribose pocket-occupying substituents. A limited numbers of compounds were made with substitution at the 7-position; however, these derivatives provided no advantage in potency or synthetic tractability compared to the 6-position analogs. Based on this observation, only analogs with substitution at the 6-position will be discussed in this report.

As shown in Table 2, analogs with piperazine substituents at the 6-position of the imidazopyridine ring system (**11-16**) were found to have <50 nM enzymatic potency. These compounds showed cellular potencies of <70 nM, with compound **13** being the only exception with near 300 nM cellular potency. Substitution at the 6-position improved microsomal stability with all of the compounds assayed having rat and human liver microsome clearance values below 100 μL/min/mg with most having values of <14 μL/min/mg.

Table 2. In vitro potency and microsomal stability of PI3Kα/mTOR inhibitors containing substituents occupying the ribose pocket.

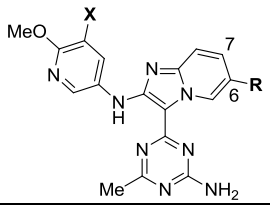

Compound	X	R	PI3Kα (K_i, nM)[a]	mTOR (IC_{50}, nM)[a]	pAKT (U87 MG) (IC_{50}, nM)[b]	Liver Microsomes (CL_{int}, μL/min/mg)[b]	
						Rat	Human
11	F	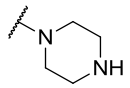	5.7	62	41	<14	<14
12	H	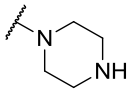	43	20	69	<14	<14
13	F	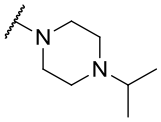	6.5	412	294	<14	<14
14	F	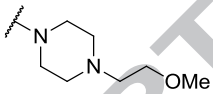	6.3	121	26	<14	28
15	H	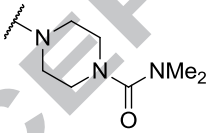	8.3	34	34	30	73
16	F	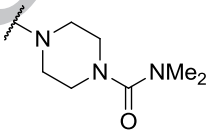	6.1	157[b]	20	<14	67
17	H	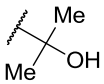	26	36	45	25	17
18	F	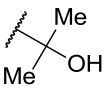	11	206	4.5	<14	<14

[a]Data represents an average of at least two determinations unless indicated otherwise. A statistical analysis of this data may be found in the supplementary material.[b]Data represents a single measurement.

Other substituents that were used to occupy the ribose pocket included tertiary alcohols, such as in compounds **17** and **18**.[36] These alcohols were comparable to the piperazine analogs in enzyme potency. While **18** was of similar potency in the enzyme assay (11 nM) to many of the piperazines, it did have the best combination of excellent cellular potency (4.5 nM) and rat and liver microsome stability (<14 μL/min/mg). The 3-fluoropyridine analog **18** demonstrated 19-fold selectivity over mTOR in contrast to compound **17** which showed less than twofold selectivity. In addition, with the incorporation of a

fluorine atom on the methoxypyridine ring, an improvement in cellular potency (**17**, 45 nM vs **18**, 4.5 nM) was obtained.

Compound **18** was potent towards the PI3Kβ, γ and δ, isoforms in the enzyme assay with K_i values of 17 nM, 5.3 nM and 0.6 nM, respectively. This lack of isoform selectivity was generally observed for the compounds described herein.

Based on its excellent potency and in vitro stability, tertiary alcohol **18**[37] was further evaluated in pharmacokinetic and pharmacodynamic (PD) studies. In rats, intravenous dosing of compound **18** demonstrated a clearance of 1.7 L/h/kg; (52% of liver blood flow) and a volume of distribution of 4.2 L/kg with a terminal elimination half-life of 6.3 hours. Compound **18** dosed orally in rats at 2 mg/kg also showed good oral bioavailability (51%) and moderate plasma exposure (AUC = 640 ng·h/mL). The in vivo activity of compound **18** was evaluated in a mouse liver pharmacodynamic assay that measured inhibition of hepatocyte growth factor (HGF)-induced AKT (Ser473) phosphorylation (Figure 3). In this assay, mice were dosed orally with compound **18** at 3, 10, and 30 mg/kg and, after 6 hours, PI3K dependent AKT phosphorylation was stimulated by HGF administration. AKT (Ser473) phosphorylation levels were measured 5 minutes after HGF administration by a quantitative electrochemiluminescence immunoassay. Imidazopyridine **18** showed significant inhibition of AKT phosphorylation at all three doses, with a maximum inhibition of 56% at the 30 mg/kg dose. The calculated ED_{50} relative to vehicle for **18** in this study was 11 mg/kg.[38]

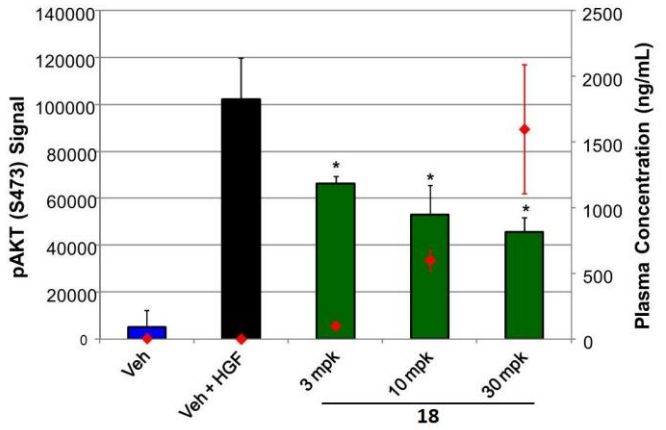

Figure 3. Inhibition of hepatocyte growth factor (HGF)-induced AKT (Ser473) phosphorylation in the liver by compound **18**. Mice were dosed orally with either vehicle alone (15% HPBCD, 2% HPMC, 1% Pluronic F68, adjusted to pH 2.2 w/MSA) or with **18**. HGF-induced AKT (Ser473) phosphorylation was measured 6 hours post-dose. Asterisks denote $p < 0.05$ compared with the vehicle/HGF group. Statistical significance was evaluated by Dunnett's method. Bars represent the average ± SD (n = 3). Red diamonds represent mean plasma concentrations.[31]

Compounds of general structure **3** in which R = H (**4**-**10**), were synthesized as shown in Scheme 1 beginning with 2-chloroimidazo[1,2-*a*]pyridine (**19**).[39] For example, through Method A, **19** underwent a Pd-catalyzed C-N coupling reaction[40] with various aryl amines to afford **20** in modest-to-good yields. Imidazopyridines **20** then advanced into Pd-catalyzed arylation reactions[41,42] with chlorotriazine **21** to install the protected amino-triazine moiety of **22**. Cleavage of the PMB protecting groups of **22** under acidic conditions afforded final compounds **4**, **7**, **9**, and **10**. Alternatively, analogs **5**, **6**, and **8** were made by Method B through initial incorporation of the triazine moiety which gave **23** followed by introduction of the aryl amine groups to give **22**. Subsequent PMB removal afforded the final compounds.

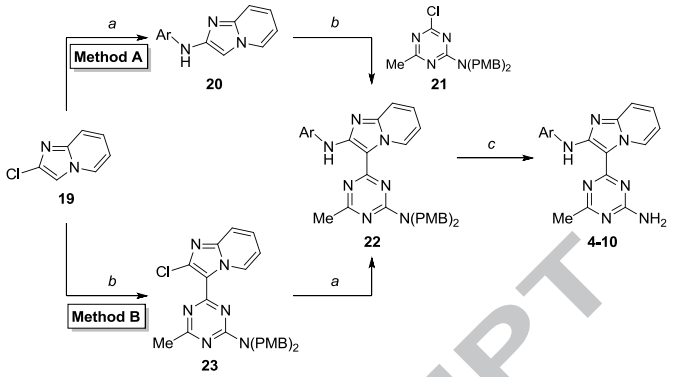

Scheme 1. Reagents and conditions: (a) Ar-NH_2, BrettPhos Precatalyst, NaOtBu, 1,4-dioxane, 90 °C, 1-16 h, 22-77%; (b) **21**, $Pd(OAc)_2$, PPh_3, K_2CO_3, 1,4-dioxane, 140 °C, 3 h, microwave, 14-85%; (c) TfOH, TFA, 25-70 °C, 1-12 h, 12-95%.

The synthesis of compounds with substituents in the 6-position of the imidazopyridine ring (**11**-**18**) began with 6-bromo-2-chloroimidazo[1,2-*a*]pyridine (**24**)[43] in which the bromine atom was utilized to incorporate the ribose pocket substituents (Schemes 2 and 3). For the preparation of compounds **11**-**16**, imidazopyridine **24** underwent a Pd-catalyzed C-N coupling reaction with N-Boc-piperazine selectively at the bromide position followed by a second Pd-catalyzed C-N coupling reaction at the chloride position with aminopyridines **25** and **26** to afford intermediates **27** and **28**, respectively. Pd-catalyzed arylation on the 5-membered ring with chlorotriazine **21** afforded **29** and **30**.

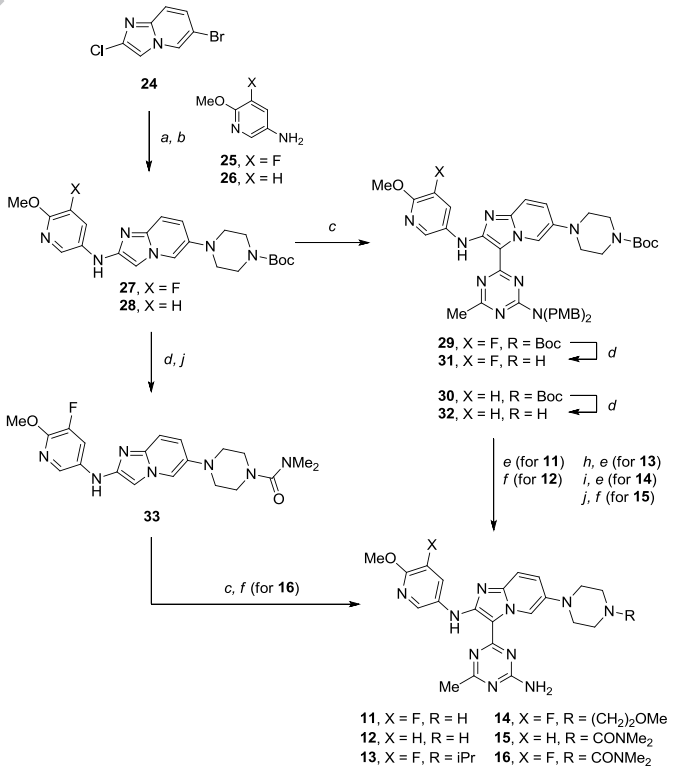

Scheme 2. Reagents and conditions: (a) *N*-Boc-piperazine, $Pd_2(dba)_3$, NaOt-Bu, *rac*-BINAP, tol., 120 °C, 30 min, microwave, 72%; (b) **25** or **26**, BrettPhos Precatalyst, NaOt-Bu, 1,4-dioxane, 90 °C, 15 h, 19-40%; (c) **21**, $Pd(OAc)_2$, PPh_3, Cs_2CO_3, NEt_3, 1,4-dioxane, 140 °C, 2 h, microwave, 63-81%; (d) TFA, CH_2Cl_2, rt, 50-77%; (e) TFA, 75 °C, 45-76%; (f) TfOH, TFA, 70 °C, 1 h, 47-97%; (g) MeI, $NaHCO_3$, 56%; (h) Acetone, $NaBH(OAc)_3$, AcOH, 82%; (i) 2-Bromoethyl methyl ether, DMF, rt, 24 h, 59%; (j) Me_2NCOCl, NEt_3, CH_2Cl_2, rt, 1 h, 50-64%.

Room temperature acidic cleavage of the Boc-protecting groups provided **31** and **32**. Cleavage of the bis-PMB protecting groups under acidic conditions at elevated temperatures afforded analogs **11** and **12**. For analogs **13-15**, the piperazine nitrogen first underwent alkylation, acylation, or reductive amination prior to cleavage of the PMB protecting groups. Piperazine urea **16** was made in a similar manner to urea **15** except that the piperazine nitrogen was deprotected and carbamolated earlier in the synthesis to afford a dimethyl urea (**27** to **33**). Arylation of **33** with chlorotriazine **21** followed by cleavage of the PMB protecting groups afforded analog **16**.

For the synthesis of analogs **17** and **18**, imidazopyridine **24** underwent a Stille coupling with tributyl(1-ethoxyvinyl)tin followed by Pd-catalyzed C-N couplings with **25** or **26** to afford, after acid-catalyzed enol ether hydrolysis, methyl ketones **34** and **35** (Scheme 3). Incorporation of the triazine moiety by Pd-catalyzed arylation afforded protected triazines **36** and **37**. Cleavage of the PMB protecting groups gave **38** and **39** and subsequent treatment of the resulting methyl ketones with methyl Grignard afforded tertiary alcohols **17** and **18**.

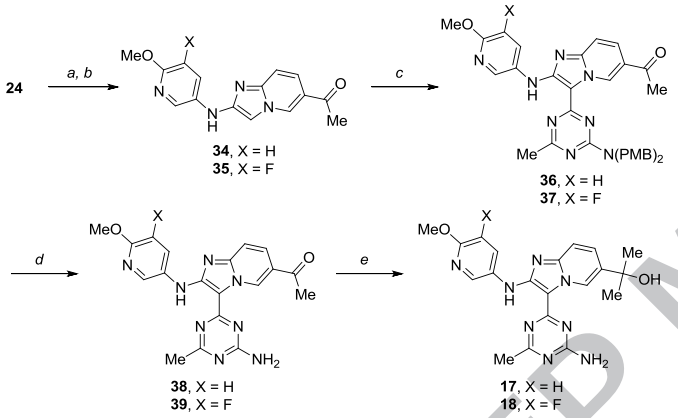

Scheme 3. Reagents and conditions: (a) tributyl(1-ethoxyvinyl)tin, $Pd(OAc)_2$, CsF, XPhos, 1,4-dioxane, 120 °C, 30 min, microwave, 79%; (b) (i) **25** or **26**, BrettPhos Precatalyst, NaOtBu, 1,4-dioxane, 90 °C, 15 h, (ii) 1 N HCl, CH_2Cl_2, 15-68%; (c) **21**, $Pd(OAc)_2$, PPh_3, Cs_2CO_3, NEt_3, 1,4-dioxane, 140 °C, 2 h, microwave, 32-88%; (d) TfOH, TFA, 70 °C, 1 h, 56-100%; (e) MeMgBr, THF, 18-86%.

In conclusion, based on benzimidazole PI3Kα/mTOR inhibitor **1**, a series of analogs were screened with an imidazopyridine core replacing the benzimidazole. Initially, various substituted aromatic rings were explored to engage the affinity pocket of PI3Kα and a 2-methoxypyridine (**4**) and 3-fluoro-2-methoxypyridine derivative (**6**) were found to give the best combination of potency and in vitro stability. Further optimization by screening a select group of substituents to occupy the ribose pocket of PI3Kα led to the identification of imidazopyridine **18** that was found to be a potent pan class I PI3K/mTOR inhibitor and was efficacious in a mouse liver pharmacodynamic assay.

Acknowledgments

We would like to thank Daniel J. Freeman for his input on in vivo pharmacology studies. The support of this research program by Randy Hungate and Rick Kendall was greatly appreciated.

References and notes

1. Toker, A. *Subcell. Biochem.* **2012**, *58*, 95.
2. Macara, I. G.; Marinetti, G. V.; Balduzzi, P. C. *Proc. Natl. Acad. Sci. U.S.A.* **1984**, *81*, 2728.
3. Sugimoto, Y.; Whitman, M.; Cantley, L. C.; Erikson, R. L. *Proc. Natl. Acad. Sci. U.S.A.* **1984**, *81*, 2117.
4. Stephens, L.; Hawkins, P. T.; Downes, C. P. *Biochem. J* **1989**, *259*, 267.
5. Engelman, J. A.; Luo, J.; Cantley, L. C. *Nat. Rev. Genet.* **2006**, *7*, 606.
6. Vivanco, I.; Sawyers, C. L. *Nat. Rev. Cancer* **2002**, *2*, 489.
7. Campbell, I. G.; Russell, S. E.; Choong, D. Y. H.; Montgomery, K. G.; Ciavarella, M. L.; Hooi, C. S. F.; Cristiano, B. E.; Pearson, R. B.; Phillips, W. A. *Cancer Res.* **2004**, *64*, 7678.
8. Samuels, Y.; Wang, Z.; Bardelli, A.; Silliman, N.; Ptak, J.; Szabo, S.; Yan, H.; Gazdar, A.; Powell, S. M.; Riggins, G. J.; Willson, J. K. V.; Markowitz, S.; Kinzler, K. W.; Vogelstein, B.; Velculescu, V. E. *Science* **2004**, *304*, 554.
9. Jeong, Y.; Kwon, D.; Hong, S. *Future Med. Chem.* **2014**, *6*, 737.
10. Joshi, M. C.; Kumar, K.; Kumar, V. *Curr. Drug Discovery Technol.* **2014**, *11*, 113.
11. Sabbah, D. A.; Brattain, M. G.; Zhong, H. *Curr. Med. Chem.* **2011**, *18*, 5528.
12. Brana, I.; Siu, L. L. *BMC Med.* **2012**, *10*, 161.
13. Fruman, D. A.; Rommel, C. *Nat. Rev. Drug Disc.* **2014**, *13*, 140.
14. Guertin, D. A.; Sabatini, D. M. *Cancer Cell* **2007**, *12*, 9.
15. Zoncu, R.; Efeyan, A.; Sabatini, D. M. *Nat. Rev. Mol. Cell Biol.* **2011**, *12*, 21.
16. PI3Kδ, which has a function in B-cell signaling pathways, has isoform-specific inhibitors in clinical trials for hematological cancers. See ref. 13.
17. Massacesi, C.; di Tomaso, E.; Fretault, N.; Hirawat, S. *Ann. N.Y. Acad. Sci.* **2013**, *1280*, 19.
18. Kurtz, J.-E.; Ray-Coquard, I. *Anticancer Res.* **2012**, *32*, 2463.
19. Pal, I.; Mandal, M. *Acta Pharmacol. Sin.* **2012**, *33*, 1441.
20. Markman, B.; Tao, J. J.; Scaltriti, M. *Curr. Pharm. Des.* **2013**, *19*, 895.
21. Yea, S. S.; Fruman, D. A. *Ann. N.Y. Acad. Sci.* **2013**, *1280*, 15.
22. Smith, A. L.; D'Angelo, N. D.; Bo, Y. Y.; Booker, S. K.; Cee, V. J.; Herberich, B.; Hong, F.-T.; Jackson, C. L. M.; Lanman, B. A.; Liu, L.; Nishimura, N.; Pettus, L. H.; Reed, A. B.; Tadesse, S.; Tamayo, N. A.; Wurz, R. P.; Yang, K.; Andrews, K. L.; Whittington, D. A.; McCarter, J. D.; San Miguel, T.; Zalameda, L.; Jiang, J.; Subramanian, R.; Mullady, E. L.; Caenepeel, S.; Freeman, D. J.; Wang, L.; Zhang, N.; Wu, T.; Hughes, P. E.; Norman, M. H. *J. Med. Chem.* **2012**, *55*, 5188.
23. Peterson, E. A.; Andrews, P. S.; Be, X.; Boezio, A. A.; Bush, T. L.; Cheng, A. C.; Coats, J. R.; Colletti, A. E.; Copeland, K. W.; DuPont, M.; Graceffa, R.; Grubinska, B.; Harmange, J.-C.; Kim, J. L.; Mullady, E. L.; Olivieri, P.; Schenkel, L. B.; Stanton, M. K.; Teffera, Y.; Whittington, D. A.; Cai, T.; La, D. S. *Bioorg. Med. Chem. Lett.* **2011**, *21*, 2064.
24. Norman, M. H.; Andrews, K. L.; Bo, Y. Y.; Booker, S. K.; Caenepeel, S.; Cee, V. J.; D'Angelo, N. D.; Freeman, D. J.; Herberich, B. J.; Hong, F.-T.; Jackson, C. L. M.; Jiang, J.; Lanman, B. A.; Liu, L.; McCarter, J. D.; Mullady, E. L.; Nishimura, N.; Pettus, L. H.; Reed, A. B.; San Miguel, T.; Smith, A. L.; Stec, M. M.; Tadesse, S.; Tasker, A.; Aidasani, D.; Zhu, X.; Subramanian, R.; Tamayo, N. A.; Wang, L.; Whittington, D. A.; Wu, B.; Wu, T.; Wurz, R. P.; Yang, K.; Zalameda, L.; Zhang, N.; Hughes, P. E. *J. Med. Chem.* **2012**, *55*, 7796.
25. Peterson, E. A.; Boezio, A. A.; Andrews, P. S.; Boezio, C. M.; Bush, T. L.; Cheng, A. C.; Choquette, D.; Coats, J. R.; Colletti, A. E.; Copeland, K. W.; DuPont, M.; Graceffa, R.; Grubinska, B.; Kim, J. L.; Lewis, R. T.; Liu, J.; Mullady, E. L.; Potashman, M. H.; Romero, K.; Shaffer, P. L.; Stanton, M. K.; Stellwagen, J. C.; Teffera, Y.; Yi, S.; Cai, T.; La, D. S. *Bioorg. Med. Chem. Lett.* **2012**, *22*, 4967.
26. The difficulty is due to limits in the generation of pure and stable protein and identifying protein constructs that are amenable to crystallization.
27. Huang, C.-H.; Mandelker, D.; Schmidt-Kittler, O.; Samuels, Y.; Velculescu, V. E.; Kinzler, K. W.; Vogelstein, B.; Gabelli, S. B.; Amzel, L. M. *Science* **2007**, *318*, 1744.
28. Amzel, L. M.; Huang, C.-H.; Mandelker, D.; Lengauer, C.; Gabelli, S. B.; Vogelstein, B. *Nat. Rev. Cancer* **2008**, *8*, 665.
29. Knight, Z. A.; Gonzalez, B.; Feldman, M. E.; Zunder, E. R.; Goldenberg, D. D.; Williams, O.; Loewith, R.; Stokoe, D.; Balla, A.; Toth, B.; Balla, T.; Weiss, W. A.; Williams, R. L.; Shokat, K. M. *Cell* **2006**, *125*, 733.

30. The experimental procedure for the mTOR assay is described in the Supplementary Material.
31. D'Angelo, N. D.; Kim, T.-S.; Andrews, K.; Booker, S. K.; Caenepeel, S.; Chen, K.; Freeman, D.; Jiang, J.; Liu, L.; McCarter, J. D.; San Miguel, T.; Mullady, E. L.; Schrag, M.; Subramanian, R.; Tang, J.; Wahl, R. C.; Wang, L.; Whittington, D. A.; Wu, T.; Xi, N.; Xu, Y.; Yakowec, P.; Zalameda, L. P.; Zhang, N.; Hughes, P.; Norman, M. H. *J. Med. Chem.* **2011**, *54*, 1789.
32. The indazole group was also selected as an affinity pocket moiety, since it has been successfully employed in this region of the enzyme by Genentech in their PI3Kα inhibitor, Pictilisib (GDC-094). See: Sarker, D.; Ang, J. E.; Baird, R.; Kristeleit, R.; Shah, K.; Moreno, V.; Clarke, P. A.; Raynaud, F. I.; Levy, G.; Ware, J. A.; Mazina, K.; Lin, R.; Wu, J.; Fredrickson, J.; Spoerke, J. M.; Lackner, M. R.; Yan, Y.; Friedman, L. S.; Kaye, S. B.; Derynck, M. K.; Workman, P.; de Bono, J. S. *Clin. Cancer Res.* **2015**, *21*, 77.
33. CL_{int} (μL/min/mg) estimated from parent compound (1 μM) remaining following a 30 min incubation in liver microsome (rat and human; 0.25 mg/mL) in potassium phosphate buffered (66.7 mM) with NADPH (1 mM) at 37 °C for 30 min. Under these conditions, a cut-off of approximately 100 μL/min/mg-protein or less was considered desirable.
34. In addition to cell potency and microsomal stability, we examined the cLogD (pH 7.4) values for the compounds listed in Table 1 (which ranged from 1.7 to 2.5). However, no correlation was observed between cLogD (pH 7.4) and activity in the U87 cellular assay (see Supplementary Information).
35. While indazole **10** showed good activity in the pAKT cellular assay and fairly good stability in human liver microsomes, it was metabolized rapidly in rat liver microsomes ($CL_{int,}$ = 175 μL/min/mg). Since the subsequent evaluation of the compounds would be in rat, this compound was not selected for further SAR development.
36. The dimethyl hydroxymethyl group was selected at this position based on some of our earlier SAR work in the pyridine series. In our efforts to identify an alternative to the piperazine sulfonamide portion of AMG 511, we were able to replace this 'ribose-pocket' group with a 2-hydroxypropyl group providing a compound that retained the favorable pharmacokinetic properties of AMG 511 and exhibited similar in vivo efficacy in a mouse liver pharmacodynamics assay. See: Lanman, B. A.; Reed, A. B.; Cee, V. J.; Hong, F.-T.; Pettus, L. H.; Wurz, R. P.; Andrews, K. L.; Jiang, J.; McCarter, J. D.; Mullady, E. L.; San Miguel, T.; Subramanian, R.; Wang, L.; Whittington, D. A.; Wu, T.; Zalameda, L.; Zhang, N.; Tasker, A. S.; Hughes, P. E.; Norman, M. H. *Bioorg. Med. Chem. Lett.* **2014**, *24*, 5630.
37. The experimental procedure for the synthesis of compound **18** is described in the Supplementary Material.
38. With a corresponding EC_{50} of 542 ng/mL and a fraction unbound (f_u) of 0.066 in mouse plasma, this results in an unbound plasma concentration of 84 nM or 7.6-fold over the IC_{50}.
39. Maxwell, B. D.; Boye, O. G.; Ohta, K. *J. Labelled Compd. Radiopharm.* **2005**, *48*, 397.
40. Fors, B. P.; Watson, D. A.; Biscoe, M. R.; Buchwald, S. L. *J. Am. Chem. Soc.* **2008**, *130*, 13552.
41. Koubachi, J.; El Kazzouli, S.; Berteina-Raboin, S.; Mouaddib, A.; Guillaumet, G. *Synlett* **2006**, 3237.
42. Liegault, B.; Lapointe, D.; Caron, L.; Vlassova, A.; Fagnou, K. *J. Org. Chem.* **2009**, *74*, 1826.
43. Bode, C.; Boezio, A.; Cheng, A. C.; Choquette, D.; Coats, J. R.; Copeland, K. W.; Huang, H.; La, D.; Lewis, R.; Liao, H.; Potashman, M.; Stellwagen, J.; Yi, S.; Norman, M.; Stec, M.; Peterson, E. A.; Graceffa, R. WO2010132598A1, 2010.